

ORIGINAL ARTICLE

Inhibitive effect of potassium methylsiliconate on hydrated swelling of montmorillonite

G.Jiang^{1,2}, Y.Xuan^{1,2*}, Y.Li^{1,2}, M.Ma^{1,2}

¹State Key Laboratory of Petroleum Resource and Prospecting, China University of Petroleum (Beijing), Changping District, Beijing 102249, (CHINA)

²MOE Key Laboratory of Petroleum Engineering, China University of Petroleum (Beijing), Changping District, Beijing 102249, (CHINA)

E-mail: hades_331@163.com

Received: 2nd September, 2013 ; Accepted: 8th October, 2013

Abstract : This paper aims at evaluating the inhibition of potassium methylsiliconate on hydrated swelling of montmorillonite and exploring the inhibitive mechanism. The result of linear swelling tests shows that potassium methylsiliconate exhibits a high performance as an effective shale inhibitor in drilling fluids. The inhibition mechanism of potassium methylsiliconate was investigated by means of a variety of methods, including Fourier transform infrared spectroscopy (FT-IR), X-ray diffraction (XRD), transmission electron microscopy (TEM), zeta potential, et al. The outstanding inhibition of potassium methylsiliconate is derived from the syn-

ergy of potassium cations and methylsiliconate anions. Methylsiliconate anions can form a hydrophobic region surrounding the individual montmorillonite particle through the adsorption on the edge sites, thus inhibiting the ingress of water into the interlayer. The primary role of potassium ions is to lead to the formation of a less hydratable structure of MMT through cation-exchange interaction.

Keywords : Potassium methylsiliconate; Montmorillonite; Hydrated swelling; Inhibition; Hydrophobic region.

INTRODUCTION

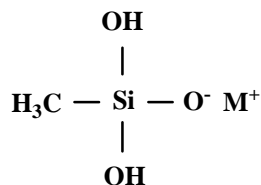
The problem of wellbore stability in water-sensitive shale formation has frustrated oil-field engineers from the beginning of the oil and gas drilling. When water-based drilling fluids encounter clay-rich shale formation, the resulting clay hydrated swelling can cause well instability often identified by solids build up in the drill-

ing fluids, tight hole, stuck drill pipes and hole enlargement, which significantly increases well construction costs, and in the worst case, can result in total abandonment of the well^[1]. Therefore, during the past 50 years, a variety of drilling fluids additives generally known as 'shale inhibitor' or 'clay stabilizer' have been developed and utilized to prevent clay from hydrated swelling. Traditionally, besides the inorganic salts such as

ORIGINAL ARTICLE

KCl^[2], the shale inhibitors are generally organic polymers or surfactants^[3], which incorporate appropriate functional groups that interact favorably with clays to reduce swelling.

Alkali metal organic siliconates that encompasses potassium methylsiliconate (PMS) and sodium methylsiliconate (SMS) is one representative of a whole series of compounds, the metal organic siliconates. The chemical structure is shown below:



(M represents alkali metal such as K, Na, Li)

Friedel and Ladenberg^[4] first made these alkali salts in their studies on alkyl silanetriols in 1870, but the first study on it was made by Meads and Kipping^[5] in 1914. According to the previous study^[6], in dilute aqueous solutions, alkali metal organic siliconate exists largely in a monomeric form $[\text{CH}_3\text{Si}(\text{OH})_2\text{O}]^- \text{M}^+$ as shown above. As silicon does not form double bonds with oxygen and silanols are easily condensed to polysiloxanes, concentrated solution of alkali metal organic siliconate probably contains polymers such as the dimer $[\text{CH}_3\text{SiOH}(\text{OM})]_2\text{O}$.

After have been used as water repellent firstly in 1950's, alkali metal organic siliconates have been applied as additive in the area of drilling fluids as well. In 1970's, SMS has been first introduced in Soviet as viscosity reducer to stabilize the properties of water-based drilling fluids^[7]. Since 2000's, SMS as viscosity reducer has become widely used in China, especially in Daqing^[8,9], Henan^[10], Huabei and Liaohe oilfield^[7].

To our knowledge, so far in the field of drilling fluids, the alkaline metal organic siliconates was mostly confined to the application as viscosity reducer additive. However, we occasionally found that PMS could act as a high-performance shale inhibitor due to the unique synergistic inhibitive effect of potassium ion and methylsiliconate anions on clay swelling in water. In this work, we report an in-deep investigation of the inhibitive effect of PMS on hydrated swelling of montmorillonite (2:1 type smectite clay). The inhibition perfor-

mance of PMS was evaluated via clay linear swelling test and the functional mechanism was analyzed through a variety of characterization methods.

EXPERIMENTAL

Reagents and materials

Potassium methylsiliconate (PMS) and sodium methylsiliconate (SMS) was obtained as 30 % aqueous solution from Xinghua Silicone Ltd., China. Montmorillonite (MMT), with cation exchange capacity of 81.3 mmol/100 g was purchased from Xinjiang Xiazijie Bentonite Inc., China. The raw samples were characterized by X-ray diffraction and FT-IR spectroscopy. Such analyses revealed that quartz, potash feldspar, anorthose, and gyp were the major impurities accompanying pristine clay. The elemental composition of the raw sample was determined by ICP-AES analysis: Si, 58.7 wt%; Al, 20.2 wt%; Na, 4.6 wt%; Fe, 8.1 wt%; Mg, 3.6 wt%; K, 3.1 wt %; Ca, 0.8 wt%; Ti 0.9 wt%. Other reagents were obtained from local reagent companies. All materials were used without further purification.

Clay linear swelling test

The linear swelling tests of MMT in inhibitor solutions were performed using CPZ-2 dual channel shale expansion instrument (Qingdao, China). 5 g MMT was placed inside the test container and condensed by hydraulic press under 10 MPa for 5 min. Then the container was fitted to the shale expansion instrument followed by pouring the inhibitor solution into it. Once the MMT contacted the inhibitor solution, the record of linear swelling of MMT in vertical direction began.

Characterizations

(a) Samples preparation

PMS aqueous solutions were prepared with different PMS concentrations (0 wt%, 0.5 wt%, 1 wt%, 3 wt%, 5 wt%, 12 wt%, 20 wt%). Then 9 g MMT was dispersed in 300 g PMS solution to make MMT/PMS aqueous suspensions with 3 wt% MMT content. The suspensions were stirred vigorously at 4000 rpm for 30 min and then shaken in a thermostated chamber at 25 °C for 16 h to reach the adsorption and hydration equilibrium.

The MMT/PMS suspensions were centrifuged for 15 min at 11000 rpm, and then the supernatant was decanted. The wet MMT on which PMS adsorbed were washed with deionized water for 5 - 6 times to eliminate the remaining PMS solutions on the surface until the pH value of the water decanted reached 7. Then, the wet MMT/PMS complex was divided into two groups. One group was directly sealed and stored at room temperature for analysis of XRD. Another group was dried in the oven at 100 °C overnight, stored being exposed to air for analysis of XRD, FT-IR, TEM, and water contact angle measurement.

(b) X-ray diffraction (XRD)

XRD patterns of the MMT/PMS complex were analyzed by D8 Advance Diffractometer (Bruker, Germany) operating at a voltage of 40 kV and a current of 40 mA, and employing Cu K α filtered radiation ($\lambda = 1.5406$ nm). Diffraction patterns were collected with 2θ angle scanning between 2 ° and 15 °.

(c) Fourier transform infrared spectroscopy (FT-IR)

FT-IR analyses of MMT/PMS were recorded by Magna-IR 560 spectrophotometer (Nicolet, U.S.A) with the wave number range 4000-400 cm⁻¹ and the resolution 4 cm⁻¹.

(d) Transmission electron microscopy (TEM)

TEM analyses were performed by a JEM-2100 transmission electron microscope (JEOL, Japan). The samples were prepared by dispersing the MMT and MMT/PMS complex into deionized water to form 0.1 wt% aqueous suspensions, and then the suspensions were ultrasonicated for 30 min. The prepared suspensions were dipped onto the amorphous carbon-coated copper TEM grids and dried under an infrared lamp.

(e) Zeta potential

Zeta potential of the MMT colloidal particles in PMS aqueous solution were performed using Zetasizer Nano ZS instrument (Malvern, U.K). The series of samples were prepared by dispersing 0.1 wt% MMT in PMS solutions with different concentration to form MMT/PMS suspensions. The suspensions were ultrasonicated for 30 min before measurements.

(f) Water contact angle

For this test, the self-supporting MMT films was prepared according to the method of Wu^[11]. The dried MMT/PMS complex was dispersed in water again to form 1 wt% suspensions. The suspensions were ultrasonicated for 30 min, and then aliquots of 10 ml suspensions were withdrawn with pipettes and distributed evenly on clean glass slides (2 cm \times 5 cm), which were placed strictly horizontal. The glass slides were left air-dried for at least one night until the smooth and thin MMT films formed, and then the films coated on the slides were peeled off for the test. Contact angle of water droplet on the MMT films was determined with the static sessile drop method using digital camera equipped on JC2000D contact angle measuring instrument (Powereach, China).

Yield point measurements

The yield points of the MMT/PMS suspensions were calculated from readings of 600 and 300 rpm (Φ_{600} and Φ_{300}) of ZNN-D6L viscometer (Qingdao, China), using following formulas from API Recommended Practice of Standard procedure for field testing drilling fluids^[12]: Yield point= $\Phi_{300} - \Phi_{600}/2$ (Pa).

RESULTS AND DISCUSSION

Inhibitive performance evaluation

The linear swelling curves of MMT immersed in deionized water and PMS solutions with different concentrations are presented in Figure 1. For all samples, the swelling curves display a similar shape with strong increase within the initial few hours followed by a relatively slower growth, exhibiting typical swelling behavior of MMT in aqueous solution. Obviously, among all the samples the MMT in deionized water swells the most and the adding of a small amount of PMS (0.5 wt%) largely reduces the swelling amount. With the further increase of PMS concentration to 7 wt%, the swelling amount of MMT is suppressed to approximately 20 % of that in deionized water, exhibiting an outstanding inhibition performance. When the concentration of PMS continues to increase from 7 wt% to 20 wt%, the swelling only changes a little, which seems to indicate the almost saturated adsorption of PMS on MMT near the concentration of 7 wt%.

ORIGINAL ARTICLE

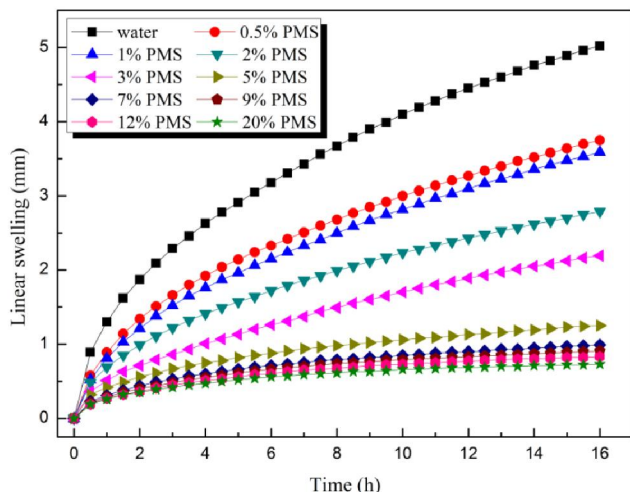


Figure 1 : Linear swelling curves of MMT in PMS solutions with different concentrations

The inhibition performance of PMS was also compared with SMS, which is shown in Figure 2. Although the swelling rates within the initial hours is parallel, the MMT in 5 wt% PMS solution reaches hydration equilibrium much earlier than in 5 wt% SMS. This could be attributed to the higher inhibitive effect of K^+ than Na^+ . Due to the proper size and low hydration energy of K^+ ^[13,14], the exchange of K^+ for interlayer cations results in a less hydratable structure of MMT. Therefore, as compared with SMS, the presence of K^+ in PMS solution that formed through ionization and hydrolysis reaction rather than Na^+ leads to an earlier hydration swelling equilibrium of MMT, which is undoubtedly beneficial for maintaining wellbore stability.

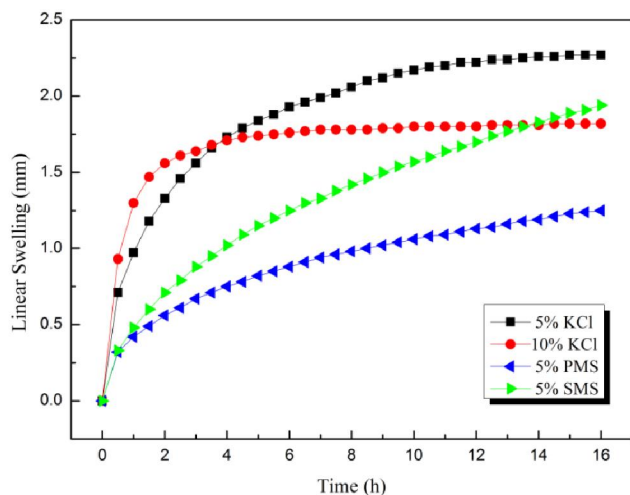


Figure 2 : Linear swelling curves of MMT in PMS, SMS and KCl solutions

Another phenomenon shown in Figure 2 that cannot be ignored is that, before reaching equilibrium, the swelling of MMT in PMS and SMS solutions are both much slower than in KCl solutions with even higher concentration of K^+ . This illustrates that besides the K^+ , the methylsiliconate anions in PMS solution also make a significant contribution to high swelling inhibition of PMS, which will be fully discussed in the chapter of mechanism analysis. For this reason, the high inhibition of PMS could be ascribed to the synergy of K^+ and methylsiliconate anions. In other words, PMS functions as the mixture of SMS and KCl. The linear swelling tests of Liu^[15] have suggested that the incorporation of 3 wt% polyethylene glycol into the 7 wt% KCl was not shown to obviously improve the inhibition on clay swelling, indicating the poor synergy of polymer and KCl, probably due to the limited ability of traditional inhibitive polymers such as polyethylene glycol and polyacrylamide^[13]. Nevertheless, unlike polymer/KCl system, the synergy of K^+ and methylsiliconate anions in PMS solution is extremely effective, confirmed by the fact that the inhibition of PMS is much stronger than both the SMS and KCl with the same concentration.

Functional mechanism analysis

In the following, the synergistic inhibitive mechanism of K^+ and methylsiliconate anions by which PMS inhibits hydrated swelling of MMT was investigated in detail through a variety of analytical methods.

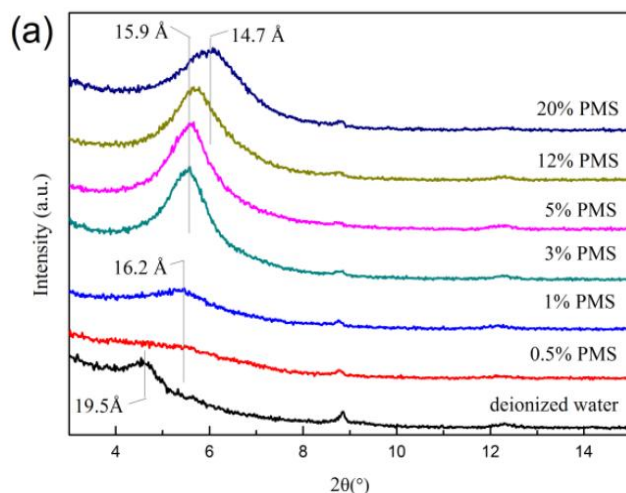
(a) X-ray diffraction

As mentioned above, K^+ in PMS solution inhibits MMT swelling through the well-known cation exchange for Na^+ in the interlayer. While in the case of methylsiliconate anion, it may function through the adsorption and interaction between silanols and siloxane surfaces of MMT.

Understanding the adsorption type of methylsiliconate anions on MMT surface is of prime importance for comprehending its inhibition mechanism. X-ray diffraction (XRD) was used to investigate the change of 001 interlayer spacing ($d_{(001)}$) of the MMT/PMS complex as compared with pristine MMT, from which we could make it clear that whether the methylsiliconate anions intercalate the interlayer or just adsorb on the external surface or the edge sites.

The evolution of the XRD patterns of the wet MMT/

PMS complex with concentration of PMS is presented in Figure 3(a). For pristine MMT, the XRD pattern displays a $d(001)$ spacing of 19.5 Å corresponding to a dominant quadric-layer hydrate stage^[16]. The addition of small amounts of PMS immediately modifies the pattern of $d(001)$. With the increase of PMS concentration up to 20 wt%, the $d(001)$ spacing decreases from 19.5 Å to 14.7 Å which is typical of a dominant double-layer stage^[17], indicating that the crystalline swelling of MMT is inhibited by PMS in aqueous suspension. The greatest change of $d(001)$ spacing occurs at the concentration ranging from 0 wt% to 5 wt%, whereas when the concentration further increases to 20 wt%, the $d(001)$ spacing changes relatively little. This is roughly consistent with the variation of swelling amount of MMT in PMS solution with increasing concentration, as shown



in Figure 4. In addition, for small PMS contents (0.5 wt% and 1 wt%), the diffraction patterns exhibit a palpable decrease of crystallinity, as judged from the width and intensity of the $d(001)$ signals. While for higher PMS concentration, the crystallinity grows up again. In the case of pure wet MMT, due to the disordering of 001 plane brought about by a large number of water molecules in the interlayer, the crystallinity is weak. When a small amount of PMS adsorb on the 001 plane, the ordering of the plane even gets much weaker, thus resulting in the decrease of crystallinity. Nonetheless, when the amount of adsorbed PMS further increases, the crystallinity gradually pick up because the largely reduction of water molecules in the interlayer offset the negative influence of the PMS adsorption on the ordering of 001 plane.

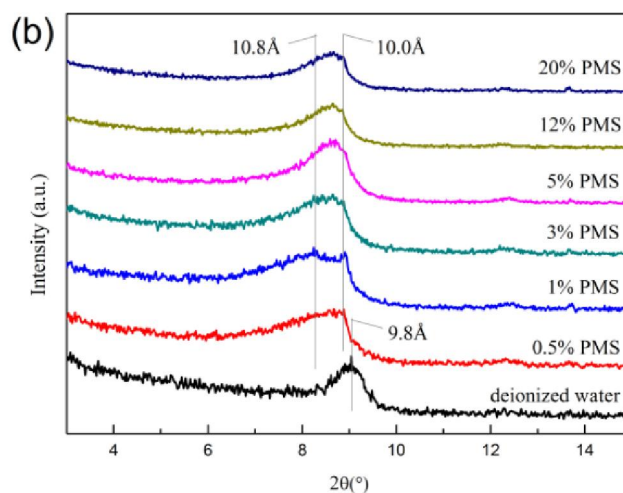


Figure 3 : XRD patterns of wet MMT/PMS complex (a) and dry MMT/PMS complex (b)

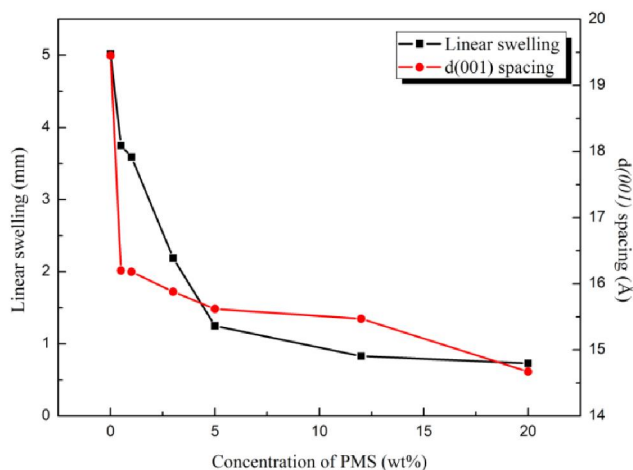


Figure 4 : Swelling amount (16 h) of MMT in PMS solutions compared with $d(001)$ spacing of MMT/PMS complex as a function of PMS concentration

Figure 3(b) presents the XRD patterns of dry MMT/PMS complex. For pristine MMT, a symmetrical peak locating at $2\theta = 8.9^\circ$ ($d(001) = 9.8$ Å) reveals a homogeneous unhydrated interlayer structure^[18]. The loading of PMS results in an asymmetric peak due to the form of heterogeneous interlayer structure. Through peak-fitting (not shown), it can be found that the heterogeneous interlayer structure contains the pristine unhydrated interlayer ($d(001) = 10.0$ Å) in combined with the interlayer on which PMS adsorbs ($d(001) = 10.8$ Å). Blachier^[19] also observed mix-interlayer structure in XRD analysis of MMT/polyamine, and attributed the heterogeneity to the intercalation of polyamine in some interlayer. In Blachier's study, increasing the polyamine loading caused the decrease of the original

ORIGINAL ARTICLE

peak intensity, and on the contrary, the increase of the new peak intensity, which indicates that the proportion of the interlayer intercalated with polyamine increases. However, for MMT/PMS, the intensity of the peak belonging to the interlayer in which PMS interact does not increase with the increasing PMS loading, seems to indicate that PMS do not intercalate the interlayer. In addition, the spacing of interlayer interacted with PMS is only approximately 0.8 \AA larger than that of pristine interlayer, far less than the full size of PMS molecule. Thus, it can be concluded that PMS molecules or methylsilicate anions do not penetrate into the internal part of the interlayer, but rather adsorb on the edge sites of MMT layers and slightly push the layers apart.

(b) Infrared spectroscopy

In order to search the inhibition mechanism, the infrared spectroscopy was used to further study the adsorption behavior of PMS on MMT. Figure 5 presents the infrared spectroscopy of MMT, PMS and MMT/PMS complex with 5 wt% PMS content. The FT-IR pattern of MMT exhibits an extremely typical characteristic of smectite group. Some of the major absorption peaks are^[20]: stretching bands of structural O-H (3625 cm^{-1}), broad stretching band of physisorbed water (3443 cm^{-1}), deformation band of water (1646 cm^{-1}), bands of Si-O stretching and Si-O-Si bending (1040 cm^{-1} and 1080 cm^{-1}). The primary absorption peaks of PMS are broad stretching band of Si-OH (3300 cm^{-1}), stretching vibration band of C-H in Si-CH₃ (2968 cm^{-1}), intense deformation bands of Si-CH₃ (1276 cm^{-1}) and deformation bands of Si-O-Si (1030 cm^{-1})^[21].

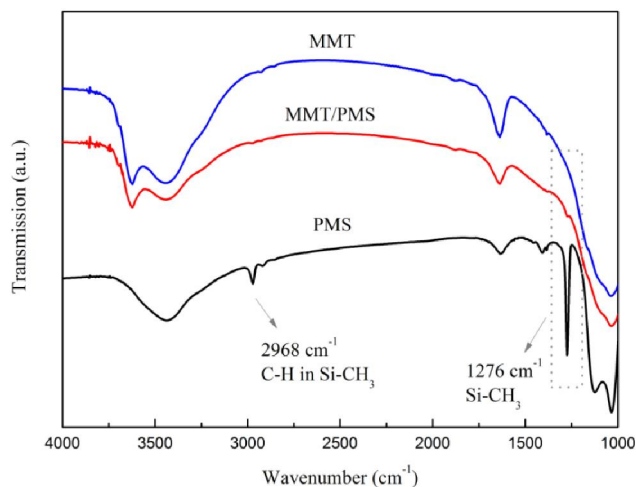


Figure 5 : FTIR spectra of MMT, PMS and MMT/PMS complex

The IR pattern of MMT/PMS is broadly similar to pure MMT, except for some inconspicuous changes. In the spectrum of PMS, the two distinct peaks belonging to Si-CH₃ are located at 2968 cm^{-1} and 1276 cm^{-1} respectively. However, for MMT/PMS, only the weak peak at 1276 cm^{-1} can be observed, indicating the small adsorption amount of PMS. The adsorption of methylsilicate anions on MMT is mainly by the formation of Si-O-Si covalent bonding^[22] between Si-OH in methylsilanol and on the edge sites of clay, rather than by H-bonding or electrostatic interaction. Therefore, the small proportion of adsorbed PMS could be due to the low number of Si-OH^[23] located at the edge sites of the individual MMT particles. In addition, the peak assigned to the physisorbed water (1646 cm^{-1}) becomes weaker compared to the pure MMT, suggesting that water physisorbed in the interlayer is reduced by the PMS. This is in good agreement with the results of XRD analysis, further confirming that the hydrated swelling of MMT can be effectively inhibited by PMS.

(c) Transmission electron microscope

The TEM images (Figure 6) reveal different dispersion state of pristine MMT and MMT/PMS complex particles in aqueous suspensions. In general, if there were no electrolytes and the temperature is not high enough, the pristine MMT particle in aqueous suspension would be well dispersed, as shown in Figure 6(a). Whereas it is crystal clear in Figure 6(b), the plate-like MMT/PMS particles are not well dispersed in water, but stacked compactly to form very thicker and larger flakes. It indicates that after the adsorption of PMS on the edge sites and the cation exchange of K⁺ for Na⁺ in the interlayer, the hydrated swelling of MMT particles becomes very difficult, corroborating the high inhibitive performance of PMS from microscopic level.

(d) Yield point and zeta potential

The yield point of suspension reflects the intensity of the internal network structure formed by MMT particles in laminar flow. Figure 7 presents the yield point curves of MMT/PMS suspension as a function of PMS concentration, from which the influence of PMS on dispersion of the MMT colloidal particles could be indirectly investigated. The yield point has an initial decrease at PMS concentrations below 1 wt%, and a subse-

quent rebound with the concentration further increases, which is in line with the zeta potential variation of MMT in PMS solution (Figure 8). In general, some of the edge sites of pure MMT particles are positive charged due to the broken bonds. At relatively high MMT content and low electrolytes concentration, the colloidal particles may exist in flocculation state due to the forming of three-dimensional reticular structure caused by the electrostatic attraction between the positive edges sites and negative charged surface. The adding of electrolytes generally may result in the compression of the diffuse double layer and the decrease of negative zeta potential. However, for MMT in PMS solution with low concentration, compared to the compression of diffuse double layer by K^+ , the chemical adsorption of

negative charged methylsiliconate anions at the edge sites of MMT plays a more significant role, thus resulting in the increase of the number of negative charge and better dispersion of MMT particles. Therefore, the initial flocculated or aggregated MMT particles become more dispersed after the adsorption of PMS, which is the reason of the yield point decrease. However, as mentioned above, the adsorption amount of PMS is low because adsorption mainly occurs at the edge sites of MMT. Therefore, with the PMS concentration further increases, the effect of PMS adsorption is limited and the impact of K^+ becomes predominant. For this reason, the zeta potential decreases and leads to a significant increase of the yield point, indicating the flocculation of the MMT particles.

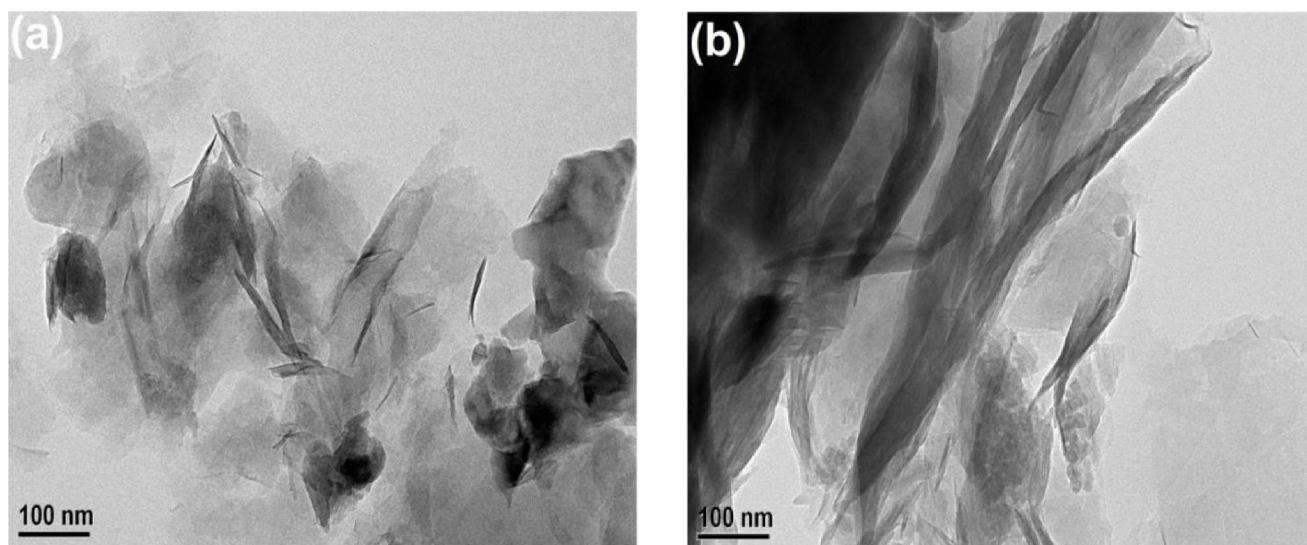


Figure 6 : TEM images of pristine MMT (a) and MMT/PMS complex with 3 wt% PMS loading (b)

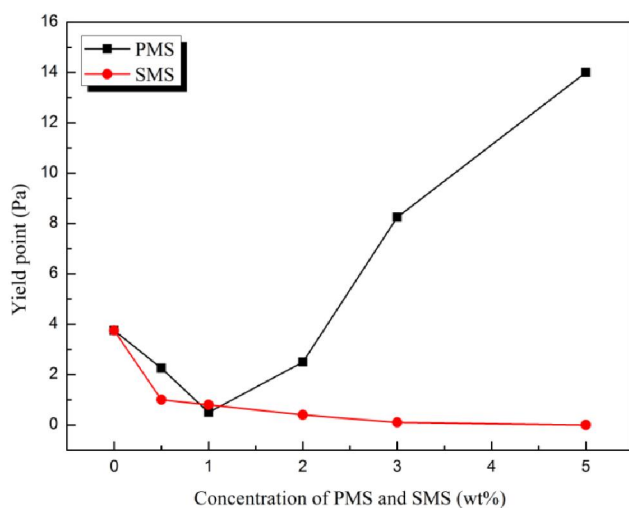


Figure 7 : Yield points of MMT/PMS and MMT/SMS suspensions as a function of concentration

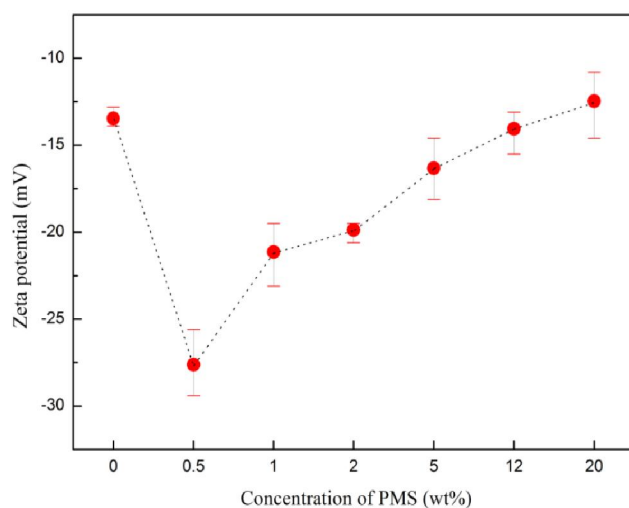


Figure 8 : Zeta potential of MMT colloidal particles in PMS solutions with different concentrations

ORIGINAL ARTICLE

In addition, also shown in Figure 7 is the yield point curve of MMT/SMS suspension that exhibits a very different pattern with that of MMT/PMS, which is a continuous declining. In view of the same concentration and valence of K^+ and Na^+ , the compression degree of diffuse double layer for MMT in PMS solution should have been closed to that in SMS solution. However, owing to the low hydrated energy of K^+ ^[13], a much thinner hydration film of MMT particles is brought about by cation-exchange adsorption of K^+ than by Na^+ . As a result, the colloidal particles in MMT/PMS suspension are more inclined to flocculate than that in MMT/SMS, which in turn indicates the much stronger inhibition effect of PMS than SMS on MMT hydrated swelling.

(e) Water contact angle

The contact angle of water on MMT/PMS film as a function of PMS loading is presented in Figure 9. The contact angle in pure MMT film is 22° , which is similar to the value measured by J. Shang^[24]. As the content of PMS increases, the contact angle has a broadly rise, which shows that the MMT/PMS film are more hydrophobic than pristine MMT film. The wettability change of the clay film is due to the adsorption of PMS. When methylsiliconate anions adsorb on the edge sites of the MMT, the outward methyl groups that are exposed to the solution produce a hydrophobic region surrounding the colloidal particle, thus preventing water from permeating into the interlayer. Moreover, at the PMS content of 1 wt%, the contact angle jumps to a very high value and drops with the increasing content. This could be explained by the change of MMT particles dispersion. As mentioned above, if the PMS concentration is at a certain low value, the particles in PMS solution are even more dispersed due to the increase of zeta potential. The roughness of the MMT/PMS film made from well-dispersed particles is relatively lower than from flocculated ones. The lower the roughness, the more hydrophobic the MMT film is. Because the MMT/PMS particles with low PMS loading of 1 wt% are well dispersed, as a consequence, the produced film is far more hydrophobic than that made from flocculated particles, reflected by the jumping of the contact angle.

(f) Summary of inhibition mechanism

According to the aforementioned analysis, the glo-

bal inhibition mechanism of PMS is available, shown in Figure 10. The strong inhibitive effect of PMS on MMT hydrated swelling can be ascribed to the synergy of the K^+ and the methylsiliconate anions. The adsorption of methylsiliconate anions at the edge sites prepares a hydrophobic region surrounding the MMT particles, thus inhibiting the ingress of water into the interlayer largely, which explains why the swelling rate of MMT in PMS solution is extremely low. With respect to K^+ , the primary role is to lead to the formation of low hydratable structure of MMT through the well-known ion-exchange interaction with interlayer cations. Due to the containing of Na^+ rather than K^+ , the inhibition of SMS is much weaker than that of PMS, therefore, SMS can only be applied as viscosity reducer additive but PMS has the potential to be a high-performance shale inhibitor in water-based drilling fluids.

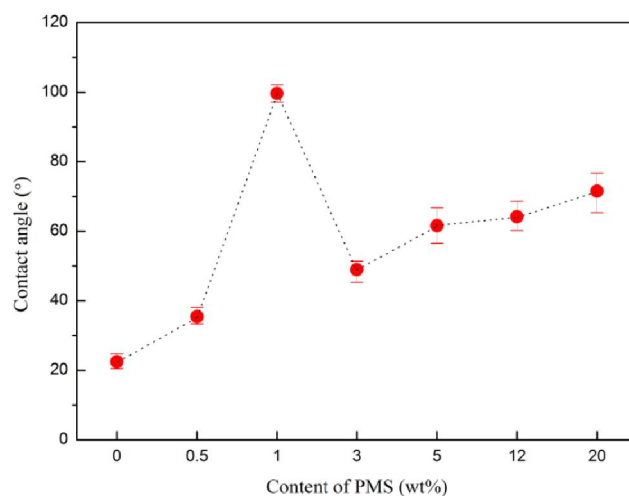


Figure 9 : Water contact angle on MMT/PMS films with different PMS loadings

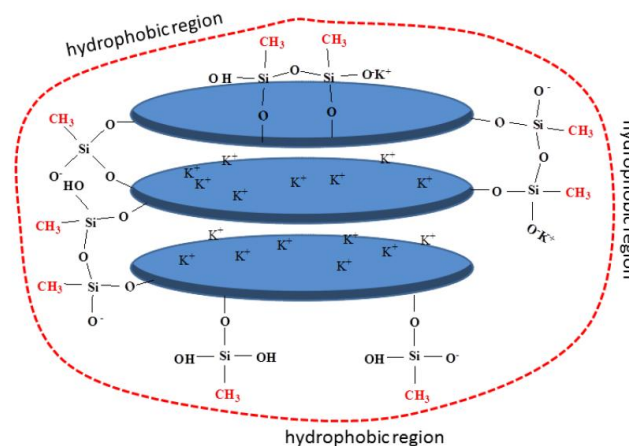


Figure 10 : Schematic diagram of inhibition mechanism of PMS

CONCLUSIONS

Unlike sodium methylsilicate that traditionally used as viscosity reducer additive, potassium methylsilicate exhibits strong inhibition on MMT hydrated swelling and has the potential to be applied as a high-performance shale inhibitor in water-based drilling fluids. According to the mechanism analysis, the outstanding inhibition effect of potassium methylsilicate on MMT swelling is due to the synergy of K^+ and methylsilicate anions. Through chemical adsorption on the edge sites rather than intercalation into the interlayer, methylsilicate anions form a hydrophobic region surrounding the MMT particle, thus inhibiting the ingress of water into the interlayer to a large degree. In the case of K^+ , due to its low hydration energy, the primary role is to lead to the formation of a less hydratable structure of MMT through cation-exchange interaction. The synergistic effect of K^+ and the methylsilicate anions explains why the inhibition performance of potassium methylsilicate is much higher than sodium methylsilicate.

ACKNOWLEDGEMENTS

We would like to thank for the financial support from National Natural Science Foundation of China (No. 51074173) and Foundation for Innovative Research Groups of the National Natural Science Foundation of China (No. 50921002) for this work.

REFERENCES

- [1] R.L.Anderson, I.Ratcliffe, H.C.Greenwell, et al.; *Earth-Sci.Rev.*, **98**, 201 (2010).
- [2] A.Patel, E.Stamatakis, S.Young; *SPE International Symposium on Oilfield Chemistry Houston, Texas*, **1** (2007).
- [3] L.Quintero; *J.Dispers Sci.Technol.*, **23**, 393 (2002).
- [4] C.Friedel, A.Ladeliberg; *Berichte der deutschen chemischen Gesellschaft*, **3**, 15 (1870).
- [5] J.A.Meads, F.S.Kipping; *J.Chem.Soc., Trans.*, **107**, 459 (1915).
- [6] S.WilliamI, A.T.Kather; *Ind.Eng.Chem.Res.*, **46**, 381 (1954).
- [7] H.P.Wang, J.Z.Lu; *Oilfield Chemistry (in chinese)*, **3**, 69 (1986).
- [8] A.H.Long, Y.X.Sun; *Journal of Daqing Petroleum Institute (in chinese)*, **26**, 28 (2002).
- [9] X.D.Liu; *Oilfield Chemistry (in chinese)*, **21**, 5 (2004).
- [10] Z.K.He, J.Li; *Drilling Fluid & Completion Fluid (in chinese)*, **26**, 31 (2009).
- [11] W.Wu; *Clays Clay Miner.*, **49**, 446 (2001).
- [12] Dept, A.P.I.P. Recommended practice standard procedure for laboratory testing drilling fluids. American Petroleum Institute, (1990).
- [13] D.E.O'Brien, M.E.Chenevert; *Journal of Petroleum Technology*, **25**, 1089 (1973).
- [14] X.D.Liu, X.C.Lu; *Angew.Chem., Int.Ed.*, **45**, 6300 (2006).
- [15] S.Liu, X.Mo, C.Zhang, D.Sun, C.Mu; *J.Dispers Sci.Technol.*, **25**, 63 (2004).
- [16] Z.Zhang, P.Low; *J.Colloid Interface Sci.*, **133**, 461 (1989).
- [17] J.Cases, I.Berend, M.Francois, J.Uriot, L.Michot, F.Thomas; *Clays Clay Miner.*, **45**, 8 (1997).
- [18] E.Ferrage, B.Lanson, B.A.Sakharov, V.A.Drits; *Am.Mineral.*, **90**, 1358 (2005).
- [19] C.Blachier, L.Michot, I.Bihannic, O.Barrès, A.Jacquet, M.Mosquet; *J.Colloid Interface Sci.*, **336**, 599 (2009).
- [20] R.Michal, V.Lenka, P.Eva; *Acta Geodyn.Geomater*, **8**, 47 (2011).
- [21] S.Y.Jing, H.J.Lee, C.K.Choi; *J.Korean Phys.Soc.*, **41**, 769 (2002).
- [22] N.N.Herrera, J.-M.Letoffe, J.-P.Reymond, E.Bourgeat-Lami; *J.Mater.Chem.*, **15**, 863 (2005).
- [23] P.F.Luckham, S.Rossi; *Adv.Colloid Interface Sci.*, **82**, 43 (1999).
- [24] J.Shang, M.Flury, J.B.Harsh, R.L.Zollars; *Colloids Surf, A*, **353**, 1 (2010).